

ASNC/JSNC JOINT SYMPOSIUM—REVIEW ARTICLE

¹²³I- Meta-Iodobenzylguanidine Imaging: From Standardization to Mortality Risk Models in Heart Failure

Kenichi Nakajima, MD, PhD

Received: May 23, 2016/Revised manuscript received: June 20, 2016/Accepted: July 4, 2016

© The Japanese Society of Nuclear Cardiology 2016

Abstract

¹²³I-meta-iodobenzylguanidine (MIBG) is a potent prognostic marker of chronic heart failure (CHF). However, inter-institutional variations due to methodological variations required minimization before ¹²³I-MIBG findings could be universally applied to the diagnosis, treatment and prognosis of CHF. Therefore, protocols including data acquisition, setting regions of interest for calculating heart-to-mediastinum ratios (HMR) and cross-calibration of HMR among institutions required standardization. A cross-calibration phantom was introduced to overcome institutional differences, and a large amount of experimental data were collected, which enabled multicenter comparisons and the creation of large-scale prognostic databases. Thereafter, cardiac mortality risk models to estimate short- and long-term (two and five years, respectively) mortality were created based on a standardized ¹²³I-MIBG HMR. The ability of these models to accurately determine prognosis is currently undergoing validation.

Keywords: Calibration phantom, Cardiac imaging, Data processing, Heart-to-mediastinum ratio, Prognosis

Ann Nucl Cardiol 2016 ; 2 (1) : 152-156

The clinical application of ¹²³I-meta-iodobenzylguanidine (MIBG) was approved in Japan during 1992 (1), and it has since become established in the guidelines of the Japanese Circulation Society as an effective means of evaluating the severity, therapeutic effects and prognosis of chronic heart failure (CHF) (2). Quantitation of uptake has supported the effectiveness of ¹²³I-MIBG in clinical practice and in research studies. The heart-to-mediastinum ratio (HMR) is a simple method in which regions of interest (ROIs) are placed on the heart and mediastinum, and then their average ratio is calculated (3). However, simplicity does not necessarily mean reliability, reproducibility or practicality among hospitals, where preferences for data acquisition and processing methods vary considerably. The varying factors among institutions that affect the stability of results include radiotracer doses administered, image acquisition protocols, ROI settings for processing (4, 5), and corrections for camera-collimator differences. Cardiac mortality risk models were also created (6), and these are addressed elsewhere in this article. However, a fluctuating HMR influenced the final prediction of cardiac

mortality, which could seriously impact decisions about patient management. Whereas minor differences in institutional preferences might be acceptable, diagnostic instability, differences in assessments of therapeutic effects and prognosis should be minimized before ¹²³I-MIBG could be universally applied. This article therefore addresses which issues involved in ¹²³I-MIBG imaging require standardization.

Administration of ¹²³I-MIBG and data acquisition

The amount of ¹²³I-MIBG (MyoMIBG; FUJIFILM RI Pharma Co. Ltd., Tokyo, Japan) administered for clinical studies in Japan is 111 MBq, which is lower than the amounts of AdreView (GE Healthcare, Little Chalfont, UK; Arlington Heights, IL, USA) applied in the USA (370 MBq) and Europe (185 MBq). Scintigraphic images were acquired as 256 × 256 matrices over 3-10 minutes in the anterior planar view. Early and late images were acquired at 15-30 minutes and 3-4 hours, respectively, after tracer administration, and energy was centered at 159 keV with a 15% or 20% window. One European proposal recommends medium-energy (ME) (4) or

doi : 10.17996/ANC.02.01.152

Kenichi Nakajima

Department of Nuclear Medicine, Kanazawa University Hospital, 13-1 Takara-machi, Kanazawa, Japan 920-8641

E-mail: nakajima@med.kanazawa-u.ac.jp

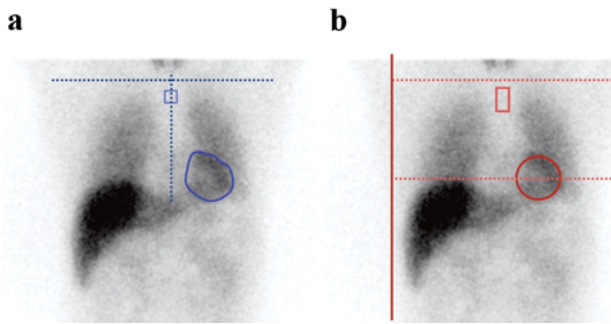


Fig. 1 Setting regions of interest

Regions of interest set according to American Society of Nuclear Medicine guidelines (a) (10) and semiautomatic software “smart-MIBG” (b) (5). Mediastinal ROI measures 7×7 pixels (a) and 10% width \times 30% height of mediastinum (b).

ME general-purpose (MEGP) collimators, but low-energy high-resolution (LEHR), low-energy general-purpose (LEGP), and low-medium-energy (LME) collimators are also popular in Japan. Single-photon emission computed tomography (SPECT) imaging also allows 360° or 180° rotation and it can score defects similar to perfusion defects (7,8). The Japanese Society Nuclear Medicine working group created normal early / late, $180^\circ / 360^\circ$ and gender-specific databases (9) that work with any software and are applicable to clinical and research purposes.

Heart-to-mediastinum ratio: ROI setting and stability

The most popular index of cardiac MIBG uptake is early and late HMR. Although the HMR is a simple average count ratio between the heart and mediastinum, the location, size and shape of the ROI results in variability. While the European Association of Nuclear Medicine Cardiovascular Committee and the European Council of Nuclear Cardiology defines no specific ROI size (4), Fig. 1 compares the ROI settings recommended by the American Society of Nuclear Cardiology (10) and the semiautomatic smartMIBG software used in Japan (5). This software needs only to point towards the center of the heart, and then a circular ROI on the heart and a rectangular ROI on the upper mediastinum are automatically determined. The mediastinal ROI was set at 10% of the body width and 30% of the height from the center of the heart to the upper border of the mediastinum. The optimal mediastinal region was automatically searched vertically to determine the minimal count on the mediastinum. The HMR remains relatively stable for three or four hours, when late images can be acquired (11, 12). A washout rate (WR) can also be calculated using the formula:

$$\text{WR (\%)} = (\text{early heart count} - \text{late heart count}) / \text{early heart count} \times 100.$$

The mediastinal count in this formula is usually subtracted from the heart count as the background, and a ¹²³I (half-life, 13 h) decay is corrected using a decay factor at three to four hours

after the initial image acquisition (correction factor of $\times 1.17$ and $\times 1.24$, respectively). Although ROI settings are generally considered reproducible (13), the semiautomatic algorithm significantly improved inter- and intra-observer variations (5).

Calibration phantom to overcome camera-collimator differences

Differences between collimators, particularly LE and ME types, cause variations in HMR measurements (14). A cross-calibration phantom was therefore designed to calibrate HMR measured in various hospitals (15,16). Two fixed HMRs were calculated from anterior and posterior planar images. Since the mathematically calculated HMR is known, two data points are obtained, and a linear regression line that passes through the coordinate (1,1) for the measured versus the reference HMR is calculated. The slope of this regression line is defined as a conversion coefficient (CC), and it is unique for each scinticamera-collimator system. We proposed unifying the HMR to the ME type of collimator, which conforms to European recommendations and is popular worldwide (4). Since the average CC of ME general-purpose collimators is 0.88 (16), any institutional HMR (HMR_i) can be standardized to MEGP-collimator condition (HMR_{std}) using the formula: $\text{HMR}_{\text{std}} = 0.88 / \text{CC}_i \times (\text{HMR}_i - 1) + 1$, where CC_i is the conversion coefficient of an institutional camera-collimator system.

The average CC of typical collimators are: 0.55, 0.65, 0.62 or 0.75, 0.83, 0.88 and 0.95 for LEHR, LEGP, extended LE general-purpose (ELEGP) with two types depending on camera, LME, MEGP and ME low penetration (MELP) collimators, respectively (16). However, the CC of the same LEHR collimator that was commonly used in the multicenter ADMIRE-HF study might have significantly varied depending on septal thickness, the size and length of the hole, as well as the camera crystals (17).

The HMR can also be calculated from images acquired using single-photon emission computed tomography (SPECT), for which custom-designed software is required to sum myocardial counts and set appropriate background regions (18). The SPECT system with solid-state detector technology, D-SPECT, has high sensitivity and resolution but it is unsuitable for obtaining planar anterior images. However, planograms comparable with planar anterior images can be reconstructed (19). Based on calculations similar to those used in conventional HMR, D-SPECT and Anger SPECT findings closely correlate. Moreover, converting the Anger HMR to the standardized HMR with a CC of 0.88, renders the HMR essentially identical, indicating that HMR derived from conventional planar images and images acquired using new SPECT cameras can be integrated (20).

Difference in collimator types did not affect WR values significantly. When the JSNM working group MIBG database

¹²³I-MIBG Standardization and Mortality Risk Models

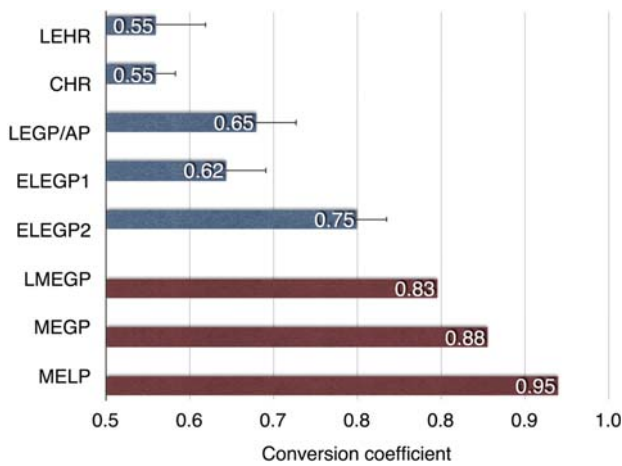


Fig. 2 Conversion coefficients for various collimators
 Average and standard deviation are shown for each collimator (16). CHR, cardiac high resolution; ELEGP1/2, extended low-energy general purpose types 1 and 2; LEHR: low-energy high resolution; LEGP/AP: low-energy general purpose/all purpose; LMEGP: low-medium energy; MEGP: medium-energy general purpose; MELP: medium-energy low penetration.

(n = 62) was analyzed (9), WRs for LE and ME/LME collimators were $13 \pm 7\%$ and $14 \pm 10\%$, respectively ($p=n.s.$), and $13 \pm 8\%$ as a whole. To utilize WR, however, application of the time-decay correction (usually 3 to 5 hours), background correction and time decay correction between early and late imaging should be unified among studies.

Application of standardization in the literature

Normal values and thresholds for predicting cardiac events significantly differ among several MIBG studies at various centers (1,17,21) and the HMR in Japanese prognostic studies is slightly higher. Although the background differs among studies according to the baseline status of patients, differences in collimators might have been involved. Japanese vendors have since attempted to optimize collimator design for the higher-energy photons emitted by ¹²³I radiopharmaceuticals that are popular in cardiac and brain studies.

For example, the optimal threshold for predicting cardiac death and lethal arrhythmia was 1.6 in the ADMIRE-HF study in which LEHR collimators were used at all participating institutions (17). When the value is converted using an average CC of 0.55, the threshold HMR can be interpreted as 2.0 with the standard ME collimator. Nakata et al. determined that a threshold of 1.74 for prognosis of CHF using an LEGP collimator (CC=0.65) (22), and it can be converted to 2.0 with the standard ME-collimator. The threshold determined from analyses of a pooled database from six Japanese hospitals (using both LEHR and LEGP collimators with an average CC of 0.6) was 1.68 (23), which was again converted to 2.0 with the standard ME collimator. Agostini et al. summarized European databases using a threshold of 1.75 (24) and LEHR, LEGP and ME collimators. When the estimated average was

0.6 based on the weighted average of their data, the corrected value was around 2.0.

To better understand the value of ¹²³I-MIBG imaging, all threshold values in the literature need to be re-evaluated, regardless of the baseline status of patients and study purpose. Larger databases for prognostic studies could be generated after original databases are created.

Application of standardized MIBG HMR to mortality risk model

Accumulating clinical evidence shows that the MIBG HMR is useful for predicting lethal cardiac events. However, actual risk for cardiac death cannot be evaluated by HMR alone. Multicenter studies such as ADMIRE-HF, a European MIBG meta-analysis, and a Japanese pooled database analysis showed that around 1.6-1.7 is the late HMR threshold for predicting a poor prognosis as alluded to above. Therefore, a cardiologist receiving for example, an MIBG report of a patient with CHF including HMR=1.55, would predict a poor prognosis. However, the significance of what the MIBG findings indicate is not exactly intuitive because cardiologists judge individual patient risk after considering several factors such as symptoms of heart failure, age, basic cardiac function, arrhythmia, medications, complications with diabetes mellitus and chronic kidney disease, and cardiac devices such as implantable cardioverter defibrillators. We therefore created cardiac mortality risk models based on multicenter pooled databases and used multivariate analysis to select the five most potent variables, namely, New York Heart Association (NYHA) functional class, age, sex, left ventricular ejection fraction (LVEF) and ¹²³I-MIBG HMR (6). To establish relatively short and long-term (two and five year, respectively) risk models, we subsequently selected the categorical variables of NYHA class (I-II and III-IV), age (<65 and ≥65 years), LVEF (<35%, 35%-50%, >50%) and HMR (<1.40, 1.40-1.69, 1.70-1.99 and ≥2.00) as variables (25). This model was applicable to both ischemic and non-ischemic etiologies of CHF. It can also be used for evaluating effectiveness of pharmacological treatment and personalized patient care in patients with heart failure (26,27).

That Japanese cohort study proceeded using LEHR and LEGP collimators between 1990 and 2009, and the cardiac risk model was generated using the averaged values of LE collimators. However, current ¹²³I-MIBG studies in Japan use LEGP, ELEGP, and LME collimators, which result in a higher HMR compared with that generated during the 1990s. Although our recommendation is standardization to the ME collimator with a conversion coefficient of 0.88, all HMRs should be converted to the LE collimator (average CC of 0.6 in the Japanese pooled database) in the internal calculation to apply this risk model to a current study. When risk models

Thresholds of late HMR				
Collimator	Severely reduced	Moderately reduced	Borderline normal	High normal
LEHR	< 1.37	1.37 - 1.63	1.64 - 1.91	≥ 1.92
LE (pooled database)	< 1.40	1.40 - 1.69	1.70 - 1.99	≥ 2.00
LEGP	< 1.43	1.43 - 1.75	1.76 - 2.07	≥ 2.08
ELEGP	< 1.50	1.50 - 1.87	1.88 - 2.24	≥ 2.25
LME	< 1.56	1.56 - 1.97	1.98 - 2.39	≥ 2.40
MEGP	< 1.59	1.59 - 2.02	2.03 - 2.46	≥ 2.47
MELP	< 1.63	1.63 - 2.10	2.11 - 2.57	≥ 2.58

Five-year risk of cardiac mortality				
LVEF (%)	Five-year risk (%)			
NYHA I - II, Age < 65y				
< 35%	24	15	9	4
35% - 50%	19	12	7	3
> 50%	14	8	5	2
NYHA I - II, Age ≥ 65y				
< 35%	32	21	14	6
35% - 50%	27	17	11	5
> 50%	20	13	8	3
NYHA III - IV, Age < 65y				
< 35%	52	38	27	14
35% - 50%	46	32	22	11
> 50%	37	25	16	8
NYHA III - IV, Age ≥ 65y				
< 35%	63	49	36	20
35% - 50%	57	43	30	16
> 50%	48	34	23	11

%/y
>10
3-10
1-3
<1

Fig. 3 Five-year cardiac mortality risk model using late HMR, NYHA functional class, LVEF and age as variables

Upper panel, threshold HMR for various collimators. Since original pooled database used for creating risk model had CC of 0.6 with thresholds of 1.4, 1.7 and 2.0, corresponding threshold values are tabulated. In the lower panel, colors of the five-year risk are: green, blue, red and purple shading, <1%, 1%-2.9%, 3%-9.9% and ≥10% risk per year, respectively. LE: low-energy; LEGP: low-energy general purpose; LEHR: low-energy high resolution; ELEGP: extended low-energy high-resolution (conversion coefficient of 0.75); LME: low-medium energy; MEGP: medium-energy general purpose; MELP: medium-energy low penetration.

were preliminarily compared between calculations based on CCs of 0.6 and 0.88, the final predicted mortality risk was nearly identical. Therefore, by combining conversion formulae among collimators, the five-year cardiac mortality risk chart became applicable to any type of collimator as shown in Fig. 3.

Conclusion

Standardization of ¹²³I-MIBG parameters, in particular HMR, plays a pivotal role in the diagnosis, treatment and prognostic estimation of CHF, whereas quantitation methods based on SPECT might progress. Cardiac mortality risk models could be more flexibly applied to various stages of CHF at any institution using standardized MIBG parameters.

Acknowledgments

This review article includes summary of multicenter cross-calibration phantom study and multicenter prognostic database created for chronic heart failure. The author appreciates collaboration of participants as indicated in references 16 and

23. The author thanks Norma Foster for editorial assistance.

Sources of funding

This work was partly supported by Grants-in-Aid for Scientific Research in Japan (PI: Kenichi Nakajima).

Conflicts of interest

K. Nakajima participates in a collaborative research project with FUJIFILM RI Pharma Co. Ltd. to develop smartMIBG software.

Reprint requests and correspondence:

Kenichi Nakajima, MD, PhD

Department of Nuclear Medicine, Kanazawa University Hospital, 13-1 Takara-machi, Kanazawa, Japan 920-8641

E-mail: nakajima@med.kanazawa-u.ac.jp

References

1. Nakajima K, Nakata T. Cardiac ¹²³I-MIBG Imaging for clinical decision making: 22-year experience in Japan. *J Nucl Med* 2015; 56 Suppl 4: 11S-9S.
2. Tamaki N. JCS Joint Working Group. Guidelines for Clinical Use of Cardiac Nuclear Medicine (Japanese Circulation Society 2010). http://www.j-circ.or.jp/guideline/pdf/JCS2010_tamaki.pdf (English digest Version in [https://www.jstage-jstgo.jp/article/circj/76/3/76_CJ-88-0019/_pdf](https://www.jstage.jstgo.jp/article/circj/76/3/76_CJ-88-0019/_pdf)). 2010.
3. Merlet P, Valette H, Dubois-Rande JL, et al. Prognostic value of cardiac metaiodobenzylguanidine imaging in patients with heart failure. *J Nucl Med* 1992; 33: 471-7.
4. Flotats A, Carrio I, Agostini D, et al. Proposal for standardization of ¹²³I-metaiodobenzylguanidine (MIBG) cardiac sympathetic imaging by the EANM Cardiovascular Committee and the European Council of Nuclear Cardiology. *Eur J Nucl Med Mol Imaging* 2010; 37: 1802-12.
5. Okuda K, Nakajima K, Hosoya T, et al. Semi-automated algorithm for calculating heart-to-mediastinum ratio in cardiac Iodine-123 MIBG imaging. *J Nucl Cardiol* 2011; 18: 82-9.
6. Nakajima K, Nakata T, Yamada T, et al. A prediction model for 5-year cardiac mortality in patients with chronic heart failure using ¹²³I-metaiodobenzylguanidine imaging. *Eur J Nucl Med Mol Imaging* 2014; 41: 1673-82.
7. Travin MI, Henzlova MJ, van Eck-Smit BL, et al. Assessment of I-mIBG and Tc-tetrofosmin single-photon emission computed tomographic images for the prediction of arrhythmic events in patients with ischemic heart failure: Intermediate severity innervation defects are associated with higher arrhythmic risk. *J Nucl Cardiol* 2016 (Epub ahead of print).
8. Dimitriu-Leen AC, Scholte AJ, Jacobson AF. ¹²³I-MIBG SPECT for Evaluation of Patients with Heart Failure. *J Nucl Med* 2015; 56 Suppl 4: 25S-30S.
9. Nakajima K. Normal values for nuclear cardiology: Japanese databases for myocardial perfusion, fatty acid and sympathetic imaging and left ventricular function. *Ann Nucl Med* 2010; 24: 125-35.
10. Henzlova MJ, Duvall WL, Einstein AJ, et al. ASNC imaging guidelines for SPECT nuclear cardiology procedures: Stress, protocols, and tracers. *J Nucl Cardiol* 2016; 23: 606-39.
11. Okuda K, Nakajima K, Sugino S, et al. Development and validation of a direct-comparison method for cardiac ¹²³I-metaiodobenzylguanidine washout rates derived from late 3-hour and 4-hour imaging. *Eur J Nucl Med Mol Imaging* 2016; 43: 319-25.
12. Dimitriu-Leen AC, Gimelli A, Al Younis I, et al. The impact of acquisition time of planar cardiac ¹²³I-MIBG imaging on the late heart to mediastinum ratio. *Eur J Nucl Med Mol Imaging* 2016; 43: 326-32.
13. Veltman CE, Boogers MJ, Meinardi JE, et al. Reproducibility of planar ¹²³I-meta-iodobenzylguanidine (MIBG) myocardial scintigraphy in patients with heart failure. *Eur J Nucl Med Mol Imaging* 2012; 39: 1599-608.
14. Verberne HJ, Feenstra C, de Jong WM, et al. Influence of collimator choice and simulated clinical conditions on ¹²³I-MIBG heart/mediastinum ratios: a phantom study. *Eur J Nucl Med Mol Imaging* 2005; 32: 1100-7.
15. Nakajima K, Matsubara K, Ishikawa T, et al. Correction of iodine-123-labeled meta-iodobenzylguanidine uptake with multi-window methods for standardization of the heart-to-mediastinum ratio. *J Nucl Cardiol* 2007; 14: 843-51.
16. Nakajima K, Okuda K, Yoshimura M, et al. Multicenter cross-calibration of I-123 metaiodobenzylguanidine heart-to-mediastinum ratios to overcome camera-collimator variations. *J Nucl Cardiol* 2014; 21: 970-8.
17. Jacobson AF, Senior R, Cerqueira MD, et al. Myocardial iodine-123 meta-iodobenzylguanidine imaging and cardiac events in heart failure. Results of the prospective ADMIRE-HF (AdreView Myocardial Imaging for Risk Evaluation in Heart Failure) study. *J Am Coll Cardiol* 2010; 55: 2212-21.
18. Chen J, Folks RD, Verdes L, et al. Quantitative I-123 mIBG SPECT in differentiating abnormal and normal mIBG myocardial uptake. *J Nucl Cardiol* 2012; 19: 92-9.
19. Bellevue D, Manrique A, Legallois D, et al. First determination of the heart-to-mediastinum ratio using cardiac dual isotope (¹²³I-MIBG/^{99m}Tc-tetrofosmin) CZT imaging in patients with heart failure: the ADRECARD study. *Eur J Nucl Med Mol Imaging* 2015; 42: 1912-9.
20. Nakajima K, Okuda K, Matsuo S, et al. The time has come to standardize ¹²³I-MIBG heart-to-mediastinum ratios including planar and SPECT methods. *Eur J Nucl Med Mol Imaging* 2016; 43: 386-8.
21. Verschure DO, Veltman CE, Manrique A, et al. For what endpoint does myocardial ¹²³I-MIBG scintigraphy have the greatest prognostic value in patients with chronic heart failure? Results of a pooled individual patient data meta-analysis. *Eur Heart J Cardiovasc Imaging* 2014; 15: 996-1003.
22. Nakata T, Miyamoto K, Doi A, et al. Cardiac death prediction and impaired cardiac sympathetic innervation assessed by MIBG in patients with failing and nonfailing hearts. *J Nucl Cardiol* 1998; 5: 579-90.
23. Nakata T, Nakajima K, Yamashina S, et al. A pooled analysis of multicenter cohort studies of ¹²³I-mIBG imaging of sympathetic innervation for assessment of long-term prognosis in heart failure. *JACC Cardiovasc Imaging* 2013; 6: 772-84.
24. Agostini D, Verberne HJ, Burchert W, et al. I-123-mIBG myocardial imaging for assessment of risk for a major cardiac event in heart failure patients: insights from a retrospective European multicenter study. *Eur J Nucl Med Mol Imaging* 2008; 35: 535-46.
25. Nakajima K, Nakata T, Matsuo S, et al. Creation of mortality risk charts using ¹²³I meta-iodobenzylguanidine heart-to-mediastinum ratio in patients with heart failure: 2- and 5-year risk models. *Eur Heart J Cardiovasc Imaging* 2016 (DOI: <http://dx.doi.org/10.1093/ehjci/jev322>; online 24 December 2015).
26. Kasama S, Toyama T, Kurabayashi M. The clinical usefulness of cardiac sympathetic nerve imaging using 123iodine-meta-iodobenzylguanidine scintigraphy to evaluate the effectiveness of pharmacological treatments in patients with heart failure *Ann Nucl Cardiol* 2015; 1 (1): 117-26.
27. Nakajima K, Jacobson AF. ¹²³I MIBG: Are there any additional roles in clinical practice of heart failure? *Ann Nucl Cardiol* 2015; 1 (1): 127-31.